Pattern Reconfigurable Antenna with Five Switchable Beams Switching in Elevation Plane

Shu-Lin Chen, *Student Member, IEEE,* Pei-Yuan Qin, *Member, IEEE,* Wei Lin, *Member, IEEE,* and Y. Jay Guo, *Fellow, IEEE*

***Abstract*—Pattern-reconfigurable antennas with multiple switchable beams, especially with both boresight and endfire directions, are highly desired for wireless communications. In this letter, a novel pattern-reconfigurable antenna is proposed that provides an efficient solution. By reconfiguring parasitic striplines placed around a radiating dipole and reflecting metal pieces under the dipole using p-i-n diodes, the antenna main beam can be switched to five directions in the elevation plane, approximately from -90° (left endfire), -45°, 0° (boresight), $+45^\circ$, to $+90^\circ$ (right endfire). The developed antenna operates at 2.45 GHz with dimensions of about $0.57\lambda\times0.45\lambda\times0.28\lambda$. An antenna prototype was fabricated and measured. For all five directional beams, The measured $|S_{11}|$ values are below -13dB, and the measured realized gains range from 5.2 to 6.5 dBi. They agree reasonably well with the simulated ones.**

***Index Terms*—Beam switching, boresight patterns, endfire patterns, pattern-reconfigurable antennas, reconfigurable antennas.**

I. Introduction

OVER the past decade, pattern-reconfigurable antennas have emerged at the forefront of antenna research due to their capabilities of enhancing the performance of wireless communication systems [1], [2].Basically, the research can be classified into three categories in terms of the radiation patterns the antenna provided. The first one is to reconfigure the main beam shape [3]-[6], such as changing the patterns between a conical one and a boresight one, which can be exploited to increase the system capacity and/or link quality in multiple-inputmultiple-output systems. The second one is to change pattern null positions [7], [8], which can alleviate the interference in the radio environment. The third one is to scan the main beam in a certain angle range. The beam scanning ability can be employed to either save energy by directing the signal toward intended users or provide larger coverage. A few novel designs have been developed that can scan the beam $\pm\alpha^\circ$ with respect to the boresight direction (α is usually less than 50) [9]-[11].

For many practical applications, a larger scanning range including endfire and boresight directions is highly desired. For example, in order to increase the range of the communication link for unmanned aerial vehicle, directional antennas with higher gains are used instead of omnidirectional antennas.

A number of pattern-reconfigurable antennas have been reported to achieve this beam agility to some extent. In [12], by loading a high impedance surface under a closely spaced microstrip parasitic array, two symmetrical endfire patterns can be reconfigured. In [13], a reconfigurable boresight radiation pattern and two endfire radiation patterns in the elevation plane can be achieved by placing parasitic strips around a driven monopole. Instead of using the parasitic strips, H-shaped resonator structures are proposed to switch the main beam between boresight and endfire directions [14]. In [15], by employing varactor diode loaded parasitic elements, two endfire beams are realized with high front-to-back ratio. It can be found that the work aforementioned can only achieve no more than three reconfigurable beams in the elevation plane including boresight and/or endfire directions. In [16], by utilizing substrate integrated waveguide structure with reconfigurable slots, the beam can be switched between six discrete directions. However, the beam cannot be steered to the boresight direction, which is always essential for wireless communications. It should be pointed out that it remains a challenge to achieve the beam switching among endfire, titled, and boresight with a single compact antenna configuration.

In this letter, a pattern-reconfigurable antenna that can produce five reconfigurable beams in half an elevation plane is presented to address the aforementioned challenge. By reconfiguring parasitic striplines placed around a radiating dipole and reflecting metal pieces under the dipole, the antenna main beam can be scanned from left endfire, left tilted, boresight, right tilted, to right endfire. The antenna dimensions are about $0.57\lambda\times0.45\lambda\times0.28\lambda$. The measured realized gains for all pattern modes range from 5.2 to 6.5 dBi.

II. Antenna Design and Analysis

A. Antenna Configuration

The geometry of the proposed pattern-reconfigurable antenna is shown in Fig. 1. It consists of two horizontally placed substrates, four supporting posts, and a vertically placed feed substrate. These three substrates are Rogers RT/Duriod 5880 laminate ($\epsilon_r = 2.2$, tan $\delta = 0.0009$). The height of the air gap between the two horizontal substrates with dimensions $L_s \times W_s \times h_s$ is h_a. The T-shaped feed substrate is centrally located that is inserted from the lower substrate to reach the upper substrate.

For the upper substrate, the metal of the top is removed and a metal radiating layer is etched on the bottom, as shown in Fig. 2. On this radiating layer, there are a radiating dipole with a length L_1 and two identical parasitic strips with a length $L_2 + 2L_3$ placed at a distance d from the center. Four diodes

Shu-Lin Chen, Pei-Yuan Qin, Wei Lin, and Y. Jay Guo are with the Global Big Data Technologies Centre, University of Technology Sydney (UTS), NSW 2007, Australia (e-mail: ShulinChen.UTS@gmail.com; Peiyuan.Qin@uts.edu.au; Wei.Lin@uts.edu.au; Jay.Guo@uts.edu.au).

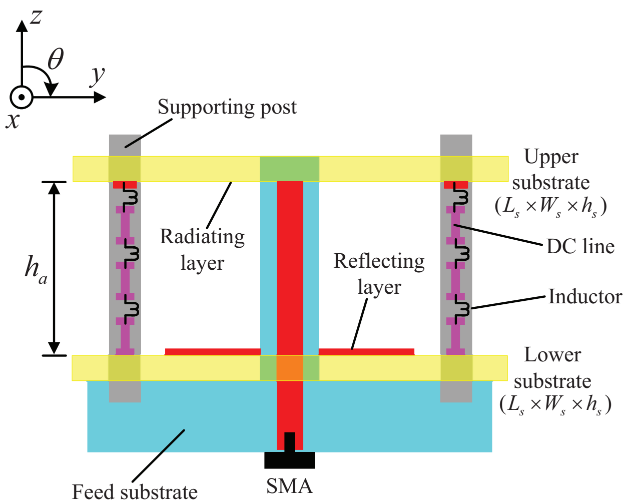

Fig. 1. Geometry of the proposed pattern reconfigurable antenna.

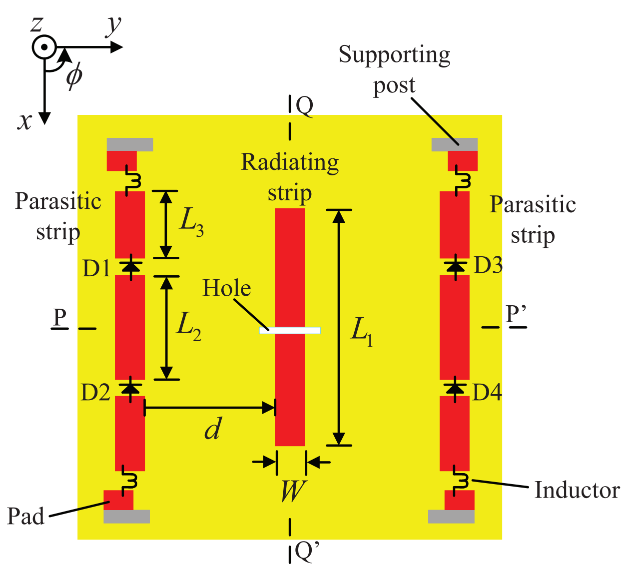

Fig. 2. Bottom view of the radiating layer.

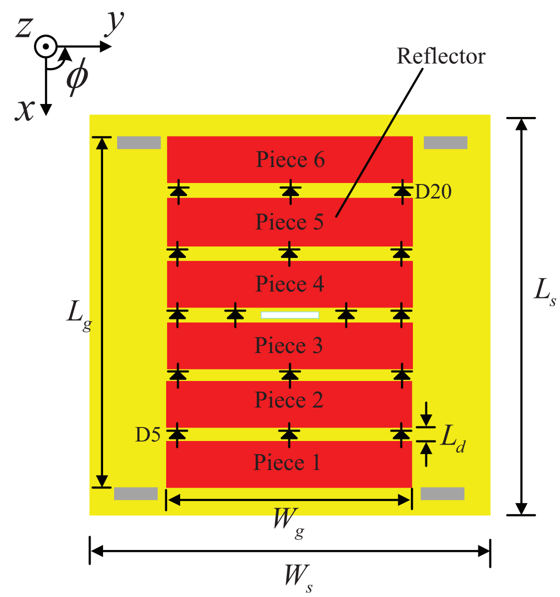

Fig. 3. Top view of the reflecting layer

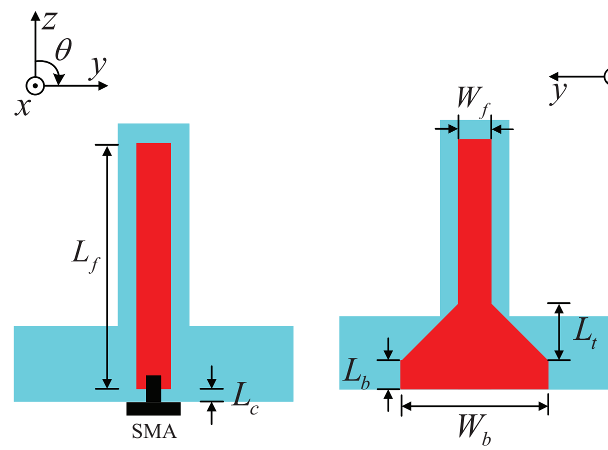

(a) (b)

Fig. 4. Configuration of the feed substrate. (a) Front view, and (b) back view.

D1-D4 are soldered across small thin slots cut on the two parasitic lines. The radiating dipole and the parasitic lines have a width W. As can be seen in Fig. 2, the whole structure of the radiating layer is symmetrical about the lines PP' and QQ'. Note that a rectangular hole is centrally drilled for inserting the feed substrate.

For the lower substrate, as shown in Fig. 3, six reflecting rectangular metal pieces are printed on the top, which is named as a reflecting layer in this letter, while the metal on the bottom of this substrate is removed. These six metal pieces are connected by 16 p-i-n diodes D5-D20 with a gap L_d. Four diodes are used between Piece 3 and Piece 4 due to the central hole for the feed substrate to go though, while three diodes are employed for other two adjacent pieces. All the diodes are oriented in the same direction along x-axis. Thus, all the 16 didoes can be switched ON/OFF simultaneously.

The feed substrate, as seen in Fig. 4, has a tapered microstrip line transferred to a coplanar stripline. With this transition, the unbalanced power from the SMA connector can be balanced at the output of the coplanar stripline, which serves as a balun feed for the radiating dipole [17]. The thickness of this feed substrate is 1 mm, and other dimensions are given in Fig. 4.

B. Pattern Reconfiguration Mechanism

The proposed pattern-reconfigurable antenna can steer its main beam in elevation plane (zy plane) to five different elevational angles. As is well known, a half-wavelength dipole antenna with a balun feed can radiate an 8-shaped pattern in the E-plane and an omnidirectional pattern in the H-plane. The main strategy of the beam scanning is to reconfigure both the parasitic striplines around the dipole printed on the upper substrate and the reflecting metal pieces printed on the lower substrate. As can be seen in Fig. 2, two diodes on either parasitic stripline are employed to reconfigure the line length. For example, when D1 and D2 are both switched ON, the length of the left parasitic line is $L_2 + 2L_3$. In this case, the

TABLE I
FIVE RECONFIGURABLE WORKING MODES

Working mode	Diode group switched ON	Pattern mode
Mode 1	D5-D20	Broadside
Mode 2	D1-D2 and D5-D20	Right tilted
Mode 3	D1-D2	Right endfire
Mode 4	D3-D4 and D5-D20	Left tilted
Mode 5	D3-D4	Left endfire

TABLE II
OPTIMIZED VALUES FOR THE PARAMETERS OF THE PROPOSED PATTERN-RECONFIGURABLE ANTENNA

Parameter	L_s	W_s	h_s	h_a	L_1	L_2
Value (mm)	70	55	1.5	28	50	25
Parameter	L_3	W	L_g	W_g	L_d	L_f
Value (mm)	12.9	2	60	30	2	39.5
Parameter	W_f	h_f	L_c	L_b	w_b	L_t
Value (mm)	3	1	2.5	6	20	7.6

parasitic line can act as the reflector for the radiating dipole. When D1 and D2 are both OFF, the length changes to be L_2. In this case, it serves as a director. The same mechanism applies for the right parasitic line. When the left one is electrically longer than the right one, the main beam will be steered to the right, and vice versa.

For the reflecting metal patches on the lower substrate, when D5-D20 are all switched ON, six pieces of the metal patches are connected with each other, thus acting as a reflector for the dipole. When D5-D20 are all OFF, the pieces are separated from each other and the operating frequency of each piece is far away from the radiating dipole. Therefore, they have little effect on the radiation pattern of the radiating dipole. Moreover, the location and number of these 16 diodes have been carefully studied to achieve good radiation performance of the antenna.

Based on the above analysis, five switchable beams can be obtained by switching the states of 20 diodes D1-D20. The corresponding biasing states of all p-i-n diodes for each beam are shown in Table I. For Mode 1, only p-i-n diodes D5-D20 are switched ON. In this case, the two parasitic lines are of the same length and there is a reflector on the lower substrate under the dipole. Therefore, the antenna radiates a boresight beam. For Mode 3, only D1 and D2 are switched ON. In this case, the left parasitic line is longer than the right one and there is no reflector under the radiating dipole, making the main beam in the H-plane be radiated to the right endfire direction ($\theta \approx 90°$). For Mode 2, D1,D2, and D5-D20 are switched ON. Compared to Mode 3, the reflector under the dipole is activated and it has an effect on the main beam direction. Therefore, the main beam is not along the right endfire direction, but steered to a right angle ($\theta \approx 45°$). The tilted angle of Mode 2 is co-determined by the reflection of the reflector on the reflecting layer and the parasitic line on the radiating layer. Specifically, one can optimize the distances of the parasitic lines d and the reflecting layer ha to the radiating dipole to achieve the requisite phase delay for the desired tilted beam angles. Similarly, a left endfire beam ($\theta \approx -90°$) and a left tilted beam ($\theta \approx -45°$) can also be achieved by switching the diodes, as shown in Table I.

C. DC feed network

As can be seen, D1 and D2 are switched ON and OFF simultaneously. To bias D1 and D2, one dc source is applied through dc lines printed on the left two supporting posts. In order to reduce the effects of dc biasing lines on the antenna radiation performance, the dc lines are broken down into small sections bridged with inductors, as can be seen in Fig. 1. To bias D3 and D4 on the right parasitic stripline, similar dc feed network is designed. Meanwhile, p-i-n diodes D5-D20 are switched ON and OFF at the same time. One dc source is applied on Piece 1 and Piece 6 to bias D5-D20.

The proposed antenna operates at 2.45 GHz. All the diodes employed in this design are BAR50-02L with 0403 surface mount packaging from Infineon Technologies. According to the datasheet, the diode can be equivalent to a resistance of 4Ω for the ON state and a resistance of 5 kΩ paralleled with a capacitor of 0.07 pF for the OFF state. All the surface inductors are Coilcraft chip inductors 0402HP-47NX_LU with the value 47 nH. They can choke RF signal at 2.45 GHz while mainting the dc continuity.

The dc power consumption of our antenna is contributed by switching on diodes for different working modes. In our antenna measurement, all the diodes are powered by a constant current supply Keithley 2230 SourceMeter. According to the datasheet of p-i-n diode BAR50-02L, a 10 mA constant current is applied to switch on one diode with a voltage of 0.95 V. Thus, for all the five working modes (Mode 1 - Mode 5) as shown in Table I, the power consumption is in the range of 0.019-0.148 W.

III. RESULTS AND DISCUSSION

The final optimized values for the parameters of the proposed pattern-reconfigurable antenna are given in Table II. An antenna prototype shown in Fig. 5(a) was fabricated and measured. Fig. 5(b)-(d) shows the simulated and measured $|S_{11}|$ values for Mode 1 - Mode 5. As can be seen, for all the working modes, the measured results agree reasonably well with the simulated ones. Some discrepancies can be found due to differences existing for 20 diodes and fabrication inaccuracies. At working frequency 2.45 GHz, measured and simulated $|S_{11}|$ values are lower than 13 dB for all five modes.

Far-field radiation patterns of the proposed antenna are measured using an NSI-700S-50 spherical near-field antenna measurement system located at the Commonwealth Scientific and Industrial Research Organization, Melbourne, Australia. Fig. 6(a)-(e) shows the simulated and measured H-plane radiation patterns at 2.45 GHz for Mode 1 - Mode 5, respectively. It can be seen that the measured results agree well with the simulated ones. Table III shows the simulated and measured gains and the measured 3 dB beamwidth. As the beamwidth for the proposed antenna is very wide, the main beam direction is calculated as the center of the 3 dB beamwidth in this letter. For example, for Mode 3, the main beam direction is at 98° for a 3dB beamwidth from 46° to 150°. Therefore, the main beam of the proposed antenna can be steered to approximate $-3°$ (boresight), $52°$, $98°$ (right endfire), $-57°$, and $-94°$ (left endfire), for Mode 1 to Mode 5, respectively, with realized gains around 5.26.5 dBi. The simulated antenna efficiencies are 93.6%, 90.0%, and 92.1% for Mode 1, Mode 2 (Mode 4), and Mode 3 (Mode 5), respectively. The losses on the diodes are in the range of 0.1-0.3 dB with regards to the realized gain of the antenna. The cross-polarization levels for all the five modes are below 10 dB.

IV. Conclusion

In this letter, a pattern-reconfigurable antenna with five switchable beams in elevation plane is proposed. The beam switching ability is achieved by reconfiguring parasitic striplines placed around the radiating dipole and reflecting metal pieces under the dipole. Five pattern modes, which are left endfire, left tilted, boresight, right tilted, and right endfire, can be obtained. The measured realized gains for all these five working modes range from 5.2 to 6.5 dBi. This antenna employs a simple structure and exhibits stable radiations, which can serve in many wireless communications systems requiring beam agilities.

References

[1] P.-Y. Qin, Y. J. Guo, A. R. Weily, and C. H. Liang, “A pattern reconfigurable U-slot antenna and its applications in MIMO systems,” *IEEE Trans. Antennas Propag.*, vol. 60, no. 2, pp. 516-528, Feb. 2012.

[2] Y. Tawk, J. Costantine, F. Makhlouf, M. Nassif, L. Geagea, and C. G. Christodoulou, “Wirelessly automated reconfigurable antenna with directional selectivity,” *IEEE Access*, vol. 5, pp. 802-811, 2017.

[3] S.-H. Chen, J.-S. Row, K.-L. Wong, “Reconfigurable square-ring patch antenna with pattern diversity,” *IEEE Trans. Antennas Propag.*, vol. 55, no. 2, pp. 472-475, Apr. 2007.

[4] C. Deng, Y. Li, Z. Zhang, and Z. Feng, “A circularly polarized pattern diversity antenna for hemispherical coverage,” *IEEE Trans. Antennas Propag.*, vol. 62, no. 10, pp. 5365-5369, Oct. 2014.

[5] N. Nguyen-Trong, L. Hall, and C. Fumeaux, “A frequency- and pattern-reconfigurable center-shorted microstrip antenna,” *IEEE Antennas Wireless Propag. Lett.*, vol. 15, pp. 1955-1958, 2016.

[6] W. Lin, H. Wong, and R. W. Ziolkowski, “Wideband pattern reconfigurable antenna with switchable broadside and conical beams,” *IEEE Antennas Wireless Propag. Lett.*, vol. 16, pp. 2638-2641, 2017.

[7] S. Yong and J. T. Bernhard, “Reconfigurable null scanning antenna with three dimensional null steer,” *IEEE Trans. Antennas Propag.*, vol. 61, no. 3, pp. 1063-1070, Mar. 2013.

[8] F. A. Dicandia, S. Genovesi, and A. Monorchio, “Null-steering antenna design using phase-shifted characteristic modes,” *IEEE Trans. Antennas Propag.*, vol. 64, no. 7, pp. 2698-2706, Jul. 2016.

[9] T. Sabapathy *et al.*, “A ground-plane-truncated, broadly steerable Yagi-Uda patch array antenna,” *IEEE Antennas Wireless Propag. Lett.*, vol. 15, pp. 1069-1072, 2016.

[10] L.-Y. Ji, Y. J. Guo, P.-Y. Qin, S. X. Gong, and R. Mittra, “A reconfigurable partially reflective surface (PRS) antenna for beam steering,” *IEEE Trans. Antennas Propag.*, vol. 63, no. 6, pp. 2387-2395, Jul. 2015.

[11] Z.-L. Lu, X.-X. Yang, G.-N. Tan, “A multidirectional pattern-reconfigurable patch antenna with CSRR on the ground,” *IEEE Antennas Wireless Propag. Lett.*, vol. 16, pp. 416-419, 2017.

[12] M. Li, S.-Q. Xiao, Z. Wang, B.-Z. Wang, “Compact surface-wave assisted beam-steerable antenna based on HIS,” *IEEE Trans. Antennas Propag.*, vol. 62, no. 7, pp. 3511-3519, Jul. 2014.

[13] X. Ding and B.-Z. Wang, “A novel wideband antenna with reconfigurable broadside and endfire patterns,” *IEEE Antennas Wireless Propag. Lett.*, vol. 12, pp. 995-998, 2013.

[14] J. Ren, X. Yang, J. Yin, and Y. Yin, “A novel antenna with reconfigurable patterns using H-shaped structures,” *IEEE Antennas Wireless Propag. Lett.*, vol. 14, pp. 915-918, 2015.

[15] F. Farzami, S. Khaledian, B. Smida, and D. Erricolo, “Pattern reconfigurable printed dipole antenna using loaded parasitic elements,” *IEEE Antennas Wireless Propag. Lett.*, vol. 16, pp. 1151-1154, 2017.

[16] L. Wu, A. J. Farrall, and P. R. Young, “Substrate integrated waveguide switched beam antennas,” *IEEE Trans. Antennas Propag.*, vol. 63, no. 5, pp. 2301-2305, May 2015.

[17] G.-Y. Chen and J.-S. Sun, “A printed dipole antenna with microstrip tapered balun,,” *Microw. Opt. Technol. Lett.*, vol. 40, no. 4, pp. 344-346, Feb 2004.

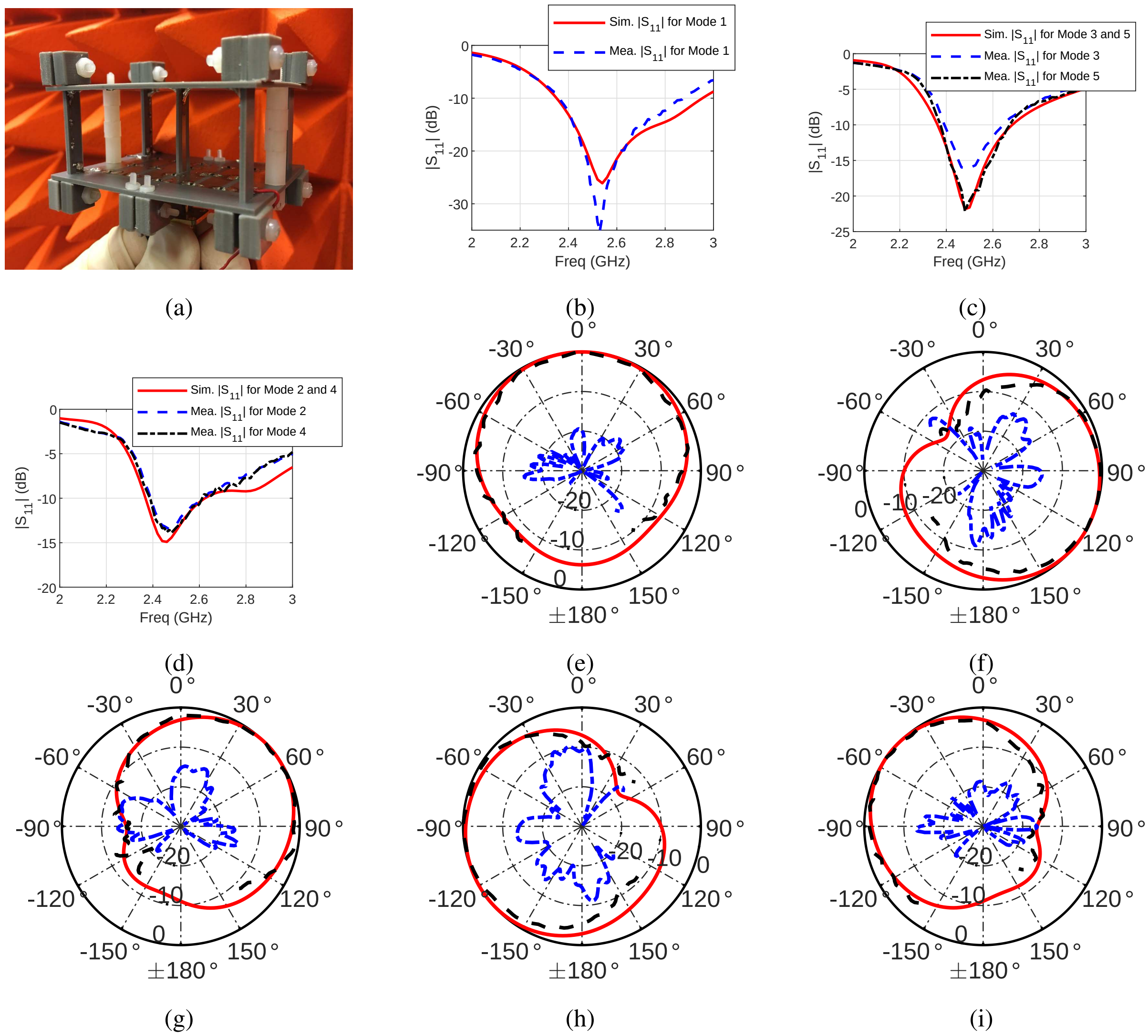

Fig. 5. (a)Antenna prototype. Simulated and measured reflection coefficients: (b) Mode 1, (c) Mode 2 and Mode 4, and (d) Mode 3 and Mode 5. Simulated and measured H-plane radiation patterns at 2.45 GHz: (e) Mode 1, (f) Mode 2, (g) Mode 3, (h) Mode 4, (i) Mode 5,.

TABLE III
SIMULATED GAINS, MEASURED GAINS AND HALF-POWER BEAMWIDTH FOR FIVE PATTERN MODES

Working Mode	Mode 1	Mode 2	Mode 3	Mode 4	Mode 5
Sim. gain (dB)	5.0	6.7	4.9	6.7	4.9
Mea. gain (dB)	5.3	6.5	5.6	6.2	5.2
Mea. half-power beamwidth	$-48° \sim 42°$	$-10° \sim 114°$	$46° \sim 150°$	$-114° \sim 0°$	$-144° \sim -44°$